fractal and fractional

Article

Shifted Fractional-Order Jacobi Collocation Method for Solving Variable-Order Fractional Integro-Differential Equation with Weakly Singular Kernel

Mohamed A. Abdelkawy [1,2,†], Ahmed Z. M. Amin [3,†], António M. Lopes [4,*,†], Ishak Hashim [3,†] and Mohammed M. Babatin [1,†]

1 Department of Mathematics and Statistics, Faculty of Science, Imam Mohammad Ibn Saud Islamic University (IMSIU), Riyadh 11432, Saudi Arabia; maohamed@imamu.edu.sa (M.A.A.); mmbabatin@imamu.edu.sa (M.M.B.)
2 Department of Mathematics, Faculty of Science, Beni-Suef University, Beni-Suef 11625, Egypt
3 Department of Mathematical Sciences, Faculty of Science, Technology, Universiti Kebangsaan Malaysia, UKM, Bangi 43600, Selangor, Malaysia; p108214@siswa.ukm.edu.my (A.Z.M.A.); ishak_h@ukm.edu.my (I.H.)
4 LAETA/INEGI, Faculty of Engineering, University of Porto, Rua Dr. Roberto Frias, 4200-465 Porto, Portugal
* Correspondence: aml@fe.up.pt
† These authors contributed equally to this work.

Abstract: We propose a fractional-order shifted Jacobi–Gauss collocation method for variable-order fractional integro-differential equations with weakly singular kernel (VO-FIDE-WSK) subject to initial conditions. Using the Riemann–Liouville fractional integral and derivative and fractional-order shifted Jacobi polynomials, the approximate solutions of VO-FIDE-WSK are derived by solving systems of algebraic equations. The superior accuracy of the method is illustrated through several numerical examples.

Keywords: variable-order fractional integro-differential equation; fractional-order shifted Jacobi polynomial; Riemann–Liouville fractional derivative; Riemann–Liouville fractional integral

Citation: Abdelkawy, M.A.; Amin, A.Z.M.; Lopes, A.M.; Hashim, I.; Babatin, M.M. Shifted Fractional-Order Jacobi Collocation Method for Solving Variable-Order Fractional Integro-Differential Equation with Weakly Singular Kernel. *Fractal Fract.* **2022**, *6*, 19. https://doi.org/10.3390/fractalfract6010019

Academic Editor: Ricardo Almeida

Received: 11 November 2021
Accepted: 27 December 2021
Published: 30 December 2021

1. Introduction

Fractional calculus [1–10] generalizes the standard differential and integral operators to non-integer orders, which, due to their non-local properties, were proven adequate for modeling and controlling systems with memory. Fractional integro-differential equations with weakly singular kernel (FIDE-WSK) are effective for modeling physical phenomena in science and engineering fields (see [11] and references therein). However, often their solutions cannot be obtained analytically and, thus, numerical techniques were developed. Nemati et al. [12] adopted a procedure based on second kind Chebyshev polynomials and operational matrix. Wang and Zhu [13] used second kind Chebyshev wavelets (SCW) and operational matrix of fractional order integration, and Zhao et al. [14] proposed collocation methods. Recently, Mokhtary [15] applied the operational Jacobi Tau method, while others developed improved distinct techniques [16–20].

Variable-order fractional integro-differential equations (V-O-FIDE) generalize the standard FIDE and obtaining their solutions is more challenging. Xu and Ertuark [21] used the finite differences method, Chen et al. [22] adopted Legendre wavelets and Sun and Zhu [23] proposed Chebyshev polynomials. We can also cite Chen et al. [24], who derived a solution for the variable-order fractional linear cable equation using polynomials of Bernstein type, and Bhrawy and Zaky [25], who used a collocation method for the two-dimensional variable-order fractional nonlinear cable equation. Tavares et al. [26] proposed to use the Caputo derivative, while other numerical techniques can be found in the literature [27–38].

Spectral methods [39–50] have been widely adopted for solving different types of equations [51–54]. Their main goal is to approximate the solution by a finite sum of basis functions, where the coefficients are selected in order to minimize the error between the exact and approximate solutions. For spectral collocation methods, the approximation must satisfy the exact solution at the collocation points, meaning that the residuals must be zero at those points.

In this paper we extend the shifted Jacobi–Gauss collocation method to solve variable-order fractional integro-differential equations with weakly singular kernel (VO-FIDE-WSK). Using the fractional-order shifted Jacobi–Gauss collocation (FSJ-G-C) method with the Riemann–Liouville fractional (R-LF) derivative and integral, and fractional-order shifted Jacobi polynomials (FO-SJP), we reduce the original problem to N algebraic equations that, together with the initial conditions, yield a system of $N+1$ equations. We apply the technique to solve several examples and prove its efficiency and accuracy.

The structure of the paper is presented in the sequel. Section 2 briefly introduces some concepts of fractional calculus and FO-SJP. Sections 3 and 4 present the new algorithm for solving VO-FIDE-WSK subject to initial and to nonlocal boundary conditions, respectively. Section 5 applies the method to some problems and illustrates its accuracy and effectiveness. Section 6 discusses the results obtained. Finally, Section 7 outlines the conclusions.

2. Mathematical Preliminaries

2.1. Basic Tools

We recall the Riemann–Liouville definitions of fractional integral and derivative of constant and variable-order, $\delta > 0$ and $\delta(t) > 0$.

Definition 1. *The R-LF integral operator I^{δ} is:*

$$I^{\delta}\psi(t) = \frac{1}{\Gamma(\delta)}\int_0^t (t-\zeta)^{\delta-1}\psi(\zeta)d\zeta, \quad \delta > 0, \quad x > 0, \quad I^0\psi(t) = \psi(t), \tag{1}$$

which satisfies:

$$I^{\gamma}I^{\delta}\psi(t) = I^{\gamma+\delta}\psi(t), \qquad I^{\gamma}I^{\delta}\psi(t) = I^{\delta}I^{\gamma}\psi(t), \qquad I^{\delta}t^{\rho} = \frac{\Gamma(\rho+1)}{\Gamma(\rho+1+\delta)}\,t^{\rho+\delta}, \tag{2}$$

where $\Gamma(\delta) = \int_0^{\infty} t^{\delta-1}e^{-t}dt$.

Definition 2. *The R-LF derivative operator D^{δ} is:*

$$D^{\delta}\psi(t) = \frac{1}{\Gamma(m-\delta)}\frac{d^m}{dt^m}\left(\int_0^t (t-s)^{m-\delta-1}\psi(s)ds\right), \quad m-1 < \delta \le m,\ t > 0, \tag{3}$$

where m stands for the ceiling function applied on δ.

Definition 3. *The R-LF integral operator of variable order $I^{\delta(t)}$ is:*

$$I^{\delta(t)}\psi = \frac{1}{\Gamma(\delta(t))}\int_0^t (t-s)^{\delta(t)-1}\psi(s)ds. \tag{4}$$

Definition 4. *The R-LF derivative operator of variable order [55,56] $D^{\delta(t)}$ is:*

$$D^{\delta(t)}\psi(t) = \frac{1}{\Gamma(m-\delta(t))}\left[\frac{d^m}{d\tau^m}\int_0^{\tau} (\tau-s)^{m-\delta(t)-1}\psi(s)ds\right]_{\tau=t}, \quad m-1 < \delta(t) \le m,\ t > 0. \tag{5}$$

2.2. The Shifted Jacobi Polynomials

Considering the properties of the Jacobi polynomials, $\mathcal{P}_k^{(\sigma,\rho)}(t)$, we can write [57,58]:

$$\mathcal{P}_{k+1}^{(\sigma,\rho)}(t) = (a_k^{(\sigma,\rho)} t - b_k^{(\sigma,\rho)})\mathcal{P}_k^{(\sigma,\rho)}(t) - c_k^{(\sigma,\rho)}\mathcal{P}_{k-1}^{(\sigma,\rho)}(t), \quad k \geq 1,$$
$$\mathcal{P}_0^{(\sigma,\rho)}(t) = 1, \quad \mathcal{P}_1^{(\sigma,\rho)}(t) = \frac{1}{2}(\sigma+\rho+2)t + \frac{1}{2}(\sigma-\rho),$$

$$\mathcal{P}_k^{(\sigma,\rho)}(-t) = (-1)^k \mathcal{P}_k^{(\sigma,\rho)}(t), \quad \mathcal{P}_k^{(\sigma,\rho)}(-1) = \frac{(-1)^k \Gamma(k+\rho+1)}{k!\Gamma(\rho+1)}, \tag{6}$$

where the parameters $\sigma,\ \rho > -1$, $x \in [-1,1]$ and

$$a_k^{(\sigma,\rho)} = \frac{(2k+\sigma+\rho+1)(2k+\sigma+\rho+2)}{2(k+1)(k+\sigma+\rho+1)},$$
$$b_k^{(\sigma,\rho)} = \frac{(\rho^2-\sigma^2)(2k+\sigma+\rho+1)}{2(k+1)(k+\sigma+\rho+1)(2k+\sigma+\rho)},$$
$$c_k^{(\sigma,\rho)} = \frac{(k+\sigma)(k+\rho)(2k+\sigma+\rho+2)}{(k+1)(k+\sigma+\rho+1)(2k+\sigma+\rho)}.$$

The derivative of order $r \in \mathbb{N}$ of $\mathcal{P}_j^{(\sigma,\rho)}(t)$ is:

$$D^r \mathcal{P}_j^{(\sigma,\rho)}(t) = \frac{\Gamma(j+\sigma+\rho+q+1)}{2^r \Gamma(j+\sigma+\rho+1)} \mathcal{P}_{j-r}^{(\sigma+r,\rho+r)}(t). \tag{7}$$

For the shifted Jacobi polynomial $\mathcal{P}_{\mathcal{L},k}^{(\sigma,\rho)}(t) = \mathcal{P}_k^{(\sigma,\rho)}(\frac{2t}{\mathcal{L}} - 1)$, $\mathcal{L} > 0$, we have the analytic expression:

$$\begin{aligned}\mathcal{P}_{\mathcal{L},k}^{(\sigma,\rho)}(t) &= \sum_{j=0}^{k} (-1)^{k-j} \frac{\Gamma(k+\rho+1)\Gamma(j+k+\sigma+\rho+1)}{\Gamma(j+\rho+1)\Gamma(k+\sigma+\rho+1)(k-j)!j!\mathcal{L}^j} t^j \\ &= \sum_{j=0}^{k} \frac{\Gamma(k+\sigma+1)\Gamma(k+j+\sigma+\rho+1)}{j!(k-j)!\Gamma(j+\sigma+1)\Gamma(k+\sigma+\rho+1)\mathcal{L}^j} (t-\mathcal{L})^j\end{aligned} \tag{8}$$

and, therefore, it yields:

$$\begin{aligned}\mathcal{P}_{\mathcal{L},k}^{(\sigma,\rho)}(0) &= (-1)^k \frac{\Gamma(k+\rho+1)}{\Gamma(\rho+1)\, k!}, \\ \mathcal{P}_{\mathcal{L},k}^{(\sigma,\rho)}(\mathcal{L}) &= \frac{\Gamma(k+\sigma+1)}{\Gamma(\sigma+1)\, k!},\end{aligned} \tag{9}$$

$$D^r \mathcal{P}_{\mathcal{L},k}^{(\sigma,\rho)}(0) = \frac{(-1)^{k-r}\Gamma(k+\rho+1)(k+\sigma+\rho+1)_r}{L^r \Gamma(k-r+1)\Gamma(r+\rho+1)}, \tag{10}$$

$$D^r \mathcal{P}_{\mathcal{L},k}^{(\sigma,\rho)}(\mathcal{L}) = \frac{\Gamma(k+\sigma+1)(k+\sigma+\rho+1)_r}{L^r \Gamma(k-r+1)\Gamma(r+\sigma+1)}, \tag{11}$$

$$D^r \mathcal{P}_{\mathcal{L},k}^{(\sigma,\rho)}(t) = \frac{\Gamma(r+k+\sigma+\rho+1)}{\mathcal{L}^r \Gamma(k+\sigma+\rho+1)} \mathcal{P}_{\mathcal{L},k-r}^{(\sigma+r,\rho+r)}(t). \tag{12}$$

Taking $w_{\mathcal{L}}^{(\sigma,\rho)}(t) = (\mathcal{L}-t)^\sigma t^\rho$, the inner product and norm in the weighted space $L^2_{w_{\mathcal{L}}^{(\sigma,\rho)}}[0,\mathcal{L}]$ are:

$$(u,v)_{w_{\mathcal{L}}^{(\sigma,\rho)}} = \int_0^{\mathcal{L}} u(t)\, v(t)\, w_{\mathcal{L}}^{(\sigma,\rho)}(t)\, dt, \quad \|v\|_{w_{\mathcal{L}}^{(\sigma,\rho)}} = (v,v)^{\frac{1}{2}}_{w_{\mathcal{L}}^{(\sigma,\rho)}}. \tag{13}$$

A complete $L^2_{w^{(\sigma,\rho)}_{\mathcal{L}}}[0,\mathcal{L}]$-orthogonal system is made of a set of shifted Jacobi polynomials, where:

$$\|\mathcal{P}^{(\sigma,\rho)}_{\mathcal{L},k}\|^2_{w^{(\sigma,\rho)}_{\mathcal{L}}} = \left(\frac{\mathcal{L}}{2}\right)^{\sigma+\rho+1} h^{(\sigma,\rho)}_k = h^{(\sigma,\rho)}_{\mathcal{L},k}. \tag{14}$$

Let the nodes and Christoffel numbers of the standard Jacobi–Gauss interpolation in the interval $[-1,1]$ be denoted by $t^{(\sigma,\rho)}_{\mathcal{N},j}$ and $\varpi^{(\sigma,\rho)}_{\mathcal{N},j}$, $0 \leqslant j \leqslant \mathcal{N}$, respectively. For the shifted Jacobi–Gauss interpolation in the interval $[0,\mathcal{L}]$ we have:

$$t^{(\sigma,\rho)}_{\mathcal{L},\mathcal{N},j} = \frac{\mathcal{L}}{2}(t^{(\sigma,\rho)}_{\mathcal{N},j} + 1),$$

$$\varpi^{(\sigma,\rho)}_{\mathcal{L},\mathcal{N},j} = \left(\frac{\mathcal{L}}{2}\right)^{\sigma+\rho+1} \varpi^{(\sigma,\rho)}_{\mathcal{N},j},\ 0 \leqslant j \leqslant \mathcal{N}.$$

For $N > 0$, $\phi \in S_{2\mathcal{N}+1}[0,\mathcal{L}]$ and the Jacobi–Gauss quadrature property, we obtain:

$$\begin{aligned}\int_0^{\mathcal{L}} (\mathcal{L}-t)^{\sigma} t^{\rho} \phi(t) dt &= \left(\frac{\mathcal{L}}{2}\right)^{\sigma+\rho+1} \int_{-1}^{1} (1-t)^{\sigma}(1+t)^{\rho} \phi\left(\frac{\mathcal{L}}{2}(t+1)\right) dt \\ &= \left(\frac{\mathcal{L}}{2}\right)^{\sigma+\rho+1} \sum_{j=0}^{\mathcal{N}} \varpi^{(\sigma,\rho)}_{\mathcal{N},j} \phi\left(\frac{\mathcal{L}}{2}(t^{(\sigma,\rho)}_{\mathcal{N},j} + 1)\right) \\ &= \sum_{j=0}^{\mathcal{N}} \varpi^{(\sigma,\rho)}_{\mathcal{L},\mathcal{N},j} \phi\left(t^{(\sigma,\rho)}_{\mathcal{L},\mathcal{N},j}\right).\end{aligned} \tag{15}$$

2.3. Fractional-Order Shifted Jacobi Polynomials

We present some results related with FO-SJP.

Definition 5. *The FO-SJP are given by:*

$$\mathcal{P}^{(\sigma,\rho,\lambda)}_{\mathcal{T},j}(t) = \mathcal{P}^{(\sigma,\rho)}_j\left(2\left(\frac{t}{\mathcal{T}}\right)^{\lambda} - 1\right),\ 0 < \lambda < 1,\ j = 0,1,\cdots,\ 0 \leq t \leq \mathcal{T}. \tag{16}$$

Theorem 1. *For $\mathcal{W}^{(\sigma,\rho,\lambda)}_{\mathcal{T},f}(t) = \lambda(\mathcal{T}^{\lambda} - t^{\lambda})^{\sigma} t^{\lambda\rho+\lambda-1}$, the set of FO-SJP forms a complete $L^2_{\mathcal{W}^{(\sigma,\rho,\lambda)}_f}[0,\mathcal{T}]$-orthogonal system:*

$$\int_0^{\mathcal{T}} \mathcal{P}^{(\sigma,\rho,\lambda)}_{\mathcal{T},i}(t)\, \mathcal{P}^{(\sigma,\rho,\lambda)}_{\mathcal{T},j}(t)\, \mathcal{W}^{(\sigma,\rho,\lambda)}_{\mathcal{T},f}(t)\, dx = \delta_{ij} h^{(\sigma,\rho,\lambda)}_{\mathcal{T},k}, \tag{17}$$

where $h^{(\sigma,\rho,\lambda)}_{\mathcal{T},k} = \left(\frac{\mathcal{T}}{2}^{\lambda}\right)^{\sigma+\rho+1} h^{(\sigma,\rho)}_i$.

Proof. The orthogonality of the Jacobi polynomials allows to write:

$$\int_{-1}^{1} \mathcal{P}^{(\sigma,\rho)}_i(x)\, \mathcal{P}^{(\sigma,\rho)}_j(x)\, \mathcal{W}^{(\sigma,\rho)}_f(x)\, dx = \delta_{ij} h^{(\sigma,\rho)}_i. \tag{18}$$

If we let $x = 2\left(\frac{t}{\mathcal{T}}\right)^{\lambda} - 1$, then we obtain:

$$
\begin{aligned}
&\int_{-1}^{1} \mathcal{P}_i^{(\sigma,\rho)}(x)\,\mathcal{P}_j^{(\sigma,\rho)}(x)\,\mathcal{W}_f^{(\sigma,\rho)}(x)\,dx \\
&= \frac{2\lambda}{\mathcal{T}^\lambda}\int_0^{\mathcal{T}} t^{\lambda-1}\mathcal{P}_i^{(\sigma,\rho)}\left(2\left(\frac{t}{\mathcal{T}}\right)^\lambda-1\right)\mathcal{P}_j^{(\sigma,\rho)}\left(2\left(\frac{t}{\mathcal{T}}\right)^\lambda-1\right)\mathcal{W}_f^{(\sigma,\rho)}\left(2\left(\frac{t}{\mathcal{T}}\right)^\lambda-1\right)dt \\
&= \left(\frac{2}{\mathcal{T}^\lambda}\right)^{\sigma+\rho+1}\int_0^{\mathcal{T}} \mathcal{P}_{\mathcal{T},i}^{(\sigma,\rho,\lambda)}(t)\,\mathcal{P}_{\mathcal{T},j}^{(\sigma,\rho,\lambda)}(t)\,\mathcal{W}_{\mathcal{T},f}^{(\sigma,\rho,\lambda)}(t)dt \\
&= \delta_{ij}h_i^{(\sigma,\rho)},
\end{aligned}
\tag{19}
$$

yielding:

$$
\begin{aligned}
\int_0^{\mathcal{T}} \mathcal{P}_{\mathcal{T},i}^{(\sigma,\rho,\lambda)}(t)\,\mathcal{P}_{\mathcal{T},j}^{(\sigma,\rho,\lambda)}(t)\,\mathcal{W}_{\mathcal{T},f}^{(\sigma,\rho,\lambda)}(t)\,dx &= \delta_{ij}\left(\frac{\mathcal{T}^\lambda}{2}\right)^{\sigma+\rho+1} h_i^{(\sigma,\rho)} \\
&= \delta_{ij}h_{\mathcal{T},i}^{(\sigma,\rho,\lambda)}.
\end{aligned}
\tag{20}
$$

□

Corollary 1. *Let the finite-dimensional fractional-polynomial space be denoted by $\mathcal{F}_N = \text{span}\{\mathcal{P}_{\mathcal{T},i}^{(\sigma,\rho,\lambda)} : 0 \le i \le N\}$. The orthogonality property (20), allows to express $\zeta(t) \in L^2_{\mathcal{W}_f^{(\sigma,\rho,\lambda)}}[0,\mathcal{T}]$ as:*

$$
\zeta(t) = \sum_{i=0}^{\infty}\gamma_i\mathcal{P}_{\mathcal{T},i}^{(\sigma,\rho,\lambda)}(t), \quad \gamma_i = \frac{1}{h_{\mathcal{T},k}^{(\sigma,\rho,\lambda)}}\int_0^{\mathcal{T}}\mathcal{P}_{\mathcal{T},i}^{(\sigma,\rho,\lambda)}(t)\,\zeta(t)\,\mathcal{W}_{\mathcal{T},f}^{(\sigma,\rho,\lambda)}(t)\,dt.
$$

Theorem 2. *The δ-order derivative of the FO-SJP, $D_t^\delta\mathcal{P}_{\mathcal{T},j}^{(\sigma,\rho,\lambda)}(t)$, can be expressed in terms of the FO-SJP as:*

$$
D_t^\delta\mathcal{P}_{\mathcal{T},j}^{(\sigma,\rho,\lambda)}(t) = \sum_{n=0}^{\mathcal{N}}\varepsilon_\delta^{(n,j,\sigma,\rho,\lambda)}\mathcal{P}_{\mathcal{T},n}^{(\sigma,\rho,\lambda)}(t),
\tag{21}
$$

where

$$
\varepsilon_\delta^{(n,j,\sigma,\rho,\lambda)} = \sum_{k=1}^{j}\sum_{s=0}^{n}\frac{E_k^{(\sigma,\rho,\lambda,j)}E_s^{(\sigma,\rho,\lambda,n)}}{h_{\mathcal{T},n}^{(\sigma,\rho,\lambda)}}\frac{k\lambda\Gamma(k\lambda)\Gamma(\sigma+1)\Gamma\left(k+s+\rho-\frac{\delta}{\lambda}+1\right)T^{\lambda(\sigma+\rho+k+s+1)-\delta}}{\Gamma(k\lambda-\delta+1)\Gamma\left(k+s+\sigma+\rho-\frac{\delta}{\lambda}+2\right)}.
$$

Proof. The analytical expression of $\mathcal{P}_{\mathcal{T},j}^{(\sigma,\rho,\lambda)}(t)$ is:

$$
\mathcal{P}_{\mathcal{T},j}^{(\sigma,\rho,\lambda)}(t) = \sum_{k=0}^{j}E_k^{(\sigma,\rho,\lambda,j)}t^{\lambda k},
$$

where

$$
E_k^{(\sigma,\rho,\lambda,j)} = \frac{(-1)^{j-k}(\Gamma(j+\rho+1)\Gamma(j+k+\sigma+\rho+1))}{k!(j-k)!\Gamma(k+\rho+1)\Gamma(j+\sigma+\rho+1)\mathcal{T}^{\lambda k}}.
$$

By means of Equation (3), we have:

$$D_t^{\delta}(t^{\lambda k}) = \frac{k\lambda\Gamma(k\lambda)t^{k\lambda-\delta}}{\Gamma(k\lambda-\delta+1)}$$

and, thus, if follows:

$$\begin{aligned} D_t^{\delta}(\mathcal{P}_{\mathcal{T},j}^{(\sigma,\rho,\lambda)}(t)) =& \mathcal{P}_{\mathcal{T},j}^{(\delta,\sigma,\rho,\lambda)}(t) \\ =& \sum_{k=1}^{j} E_k^{(\sigma,\rho,\lambda,j)} \frac{k\lambda\Gamma(k\lambda)t^{k\lambda-\delta}}{\Gamma(k\lambda-\delta+1)}. \end{aligned}$$

Using the Corollary 1, we can write:

$$t^{k\lambda-\delta} = \sum_{n=0}^{\mathcal{N}} b_{k,n}\mathcal{P}_{\mathcal{T},n}^{(\sigma,\rho,\lambda)}(t), \tag{22}$$

where

$$b_{k,n} = \frac{1}{h_{\mathcal{T},n}^{(\sigma,\rho,\lambda)}} \sum_{s=0}^{n} \frac{\Gamma(\sigma+1)\Gamma\left(k+s+\rho-\frac{\delta}{\lambda}+1\right)T^{\lambda(\sigma+\rho+k+s+1)-\delta}}{\Gamma\left(k+s+\sigma+\rho-\frac{\delta}{\lambda}+2\right)} E_s^{(\sigma,\rho,\lambda,n)}.$$

Thence, we conclude that:

$$D_t^{\delta}(\mathcal{P}_{\mathcal{T},j}^{(\sigma,\rho,\lambda)}(t)) = \sum_{n=0}^{\mathcal{N}} \varepsilon_{\delta}^{(n,j,\sigma,\rho,\lambda)}\mathcal{P}_{\mathcal{T},n}^{(\sigma,\rho,\lambda)}(t), \tag{23}$$

where

$$\varepsilon_{\delta}^{(n,j,\sigma,\rho,\lambda)} = \sum_{k=1}^{j} E_k^{(\sigma,\rho,\lambda,j)} \frac{k\lambda\Gamma(k\lambda)}{\Gamma(k\lambda-\delta+1)} b_{k,n}.$$

□

3. Algorithm for Solving VO-FIDE-WSK

The VO-FIDE-WSK to be solved are:

$$D^{\delta(t)}\chi(t) = \eta_1 \int_0^t \frac{\chi(s)}{(t-s)^{\alpha}}ds + \eta_2 \int_0^1 k(t,s)\chi(s)ds + h(t), \quad 0 < \alpha < 1, \tag{24}$$

with initial condition:

$$\chi(0) = d, \tag{25}$$

where $D^{\delta(t)}$ denotes the $\delta(t)$ variable-order fractional derivative, $\chi(t)$ is an unknown function and $h(t)$ is given.

The approximate solution of Equation (24) is given by:

$$\chi_N(t) = \sum_{j=0}^{N} e_j \mathcal{P}_{L,j}^{(\sigma,\rho,\lambda)}(t) \tag{26}$$

and the variable-order fractional derivative $D^{\delta(t)}$ of the approximate solution $\chi_N(t)$ is estimated as:

$$D^{\delta(t)}\chi_N(t) = \sum_{j=0}^{N} e_j D^{\delta(t)}(\mathcal{P}_{L,j}^{(\sigma,\rho,\lambda)}(t)). \tag{27}$$

Since we have:

$$D^{\delta(t)}t^{\lambda k}=\frac{1}{\Gamma(1-\delta(t))}\left[\frac{\partial}{\partial\tau}\left(\int\limits_0^{\tau}\frac{\chi^{\lambda k}}{(\tau-\chi)^{\delta(t)}}d\chi\right)\right]_{\tau=t}=\frac{t^{\lambda k-\delta(t)}\Gamma(1+\lambda k)}{\Gamma(1+\lambda k-\delta(t))}. \tag{28}$$

Then,

$$\begin{aligned}&D^{\delta(t)}\mathcal{P}_{L,j}^{(\sigma,\rho,\lambda)}(t)=\Lambda_{L,j}^{(\sigma,\rho,\lambda)}(t)\\&=\sum_{k=0}^{j}\frac{(-1)^{j-k}\,\Gamma(j+\rho+1)\,\Gamma(j+k+\sigma+\rho+1)}{\Gamma(k+\rho+1)\,\Gamma(j+\sigma+\rho+1)\,(j-k)!\,k!\,L^k}\,D^{\delta(t)}t^{\lambda k}\\&=\sum_{k=\lceil\delta(t)\rceil}^{j}\frac{(-1)^{i-k}\,\Gamma(1+\lambda k)\Gamma(j+\rho+1)\,\Gamma(j+k+\sigma+\rho+1)}{\Gamma(k+\rho+1)\Gamma(j+\sigma+\rho+1)(j-k)!k!\Gamma(\lambda k-\delta(t)+1)\,L^k}\,t^{\lambda k-\delta(t)}.\end{aligned} \tag{29}$$

Accordingly,

$$D^{\delta(t)}\chi_N(t)=\sum_{j=0}^{N}e_jD^{\delta(t)}\big(\mathcal{P}_{L,j}^{(\sigma,\rho,\lambda)}(t)\big)=\sum_{j=0}^{N}e_j\Lambda_{L,j}^{(\sigma,\rho,\lambda)}(t). \tag{30}$$

Comparing the term $\int_0^t\frac{\chi(s)}{(t-s)^{\alpha}}ds$ in Equations (1) and (24) we may write:

$$\int_0^t\frac{\chi(s)}{(t-s)^{\alpha}}ds=\Gamma(\alpha)I^{1-\alpha}\chi(t), \tag{31}$$

with the approximation of $I^{1-\alpha}\chi(t)$ as:

$$I^{1-\alpha}\chi_N(t)=\sum_{j=0}^{N}e_jI^{1-\alpha}\big(\mathcal{P}_{L,j}^{(\sigma,\rho,\lambda)}(t)\big). \tag{32}$$

Given that:

$$\begin{aligned}I^{1-\alpha}t^{\lambda k}&=\frac{1}{\Gamma(1-\alpha)}\int_0^t\frac{t^{\lambda k}}{(t-s)^{\alpha}}ds\\&=\frac{t^{\lambda k+1-\alpha}\Gamma(1+\lambda k)}{\Gamma(2+\lambda k-\alpha)},\end{aligned} \tag{33}$$

then

$$\begin{aligned}&I^{1-\alpha}\mathcal{P}_{L,j}^{(\sigma,\rho,\lambda)}(t)=\Delta_{L,j}^{(\sigma,\rho,\lambda)}(t)\\&=\sum_{k=0}^{j}\frac{(-1)^{j-k}\,\Gamma(j+\rho+1)\,\Gamma(j+k+\sigma+\rho+1)}{\Gamma(k+\rho+1)\,\Gamma(j+\sigma+\rho+1)\,(j-k)!\,k!\,L^k}\,I^{1-\alpha}t^{\lambda k}\\&=\sum_{k=\lceil\delta(t)\rceil}^{j}\frac{(-1)^{i-k}\,\Gamma(1+\lambda k)\Gamma(j+\rho+1)\,\Gamma(j+k+\sigma+\rho+1)}{\Gamma(k+\rho+1)\Gamma(j+\sigma+\rho+1)(j-k)!k!\Gamma(2+\lambda k-\alpha)\,L^k}\,t^{\lambda k+1-\alpha}.\end{aligned} \tag{34}$$

Accordingly,

$$I^{1-\alpha}\chi_N(t)=\sum_{j=0}^{N}e_jI^{1-\alpha}\big(\mathcal{P}_{L,j}^{(\sigma,\rho,\lambda)}(t)\big)=\sum_{j=0}^{N}e_j\Delta_{L,j}^{(\sigma,\rho,\lambda)}(t) \tag{35}$$

and we rewrite Equation (24) by using Equations (30) and (35) as:

$$\sum_{j=0}^{N} e_j \Lambda_{L,j}^{(\sigma,\rho,\lambda)}(t) = h(t) + \eta_1 \Gamma(\alpha) \sum_{j=0}^{N} e_j \Delta_{L,j}^{(\sigma,\rho,\lambda)}(t) + \eta_2 \int_0^1 k(t,s) \sum_{j=0}^{N} e_j \mathcal{P}_{L,j}^{(\sigma,\rho,\lambda)}(s) ds. \tag{36}$$

The FSJ-G-C technique requires that the residual of (36) be zero at the $N+1$ shifted Jacobi Gauss points. Therefore, using (26) and (36), we can rewrite (24) as:

$$\sum_{j=0}^{N} e_j \Lambda_{L,j}^{(\sigma,\rho,\lambda)}(t_{L,N,i}^{(\sigma,\rho)}) = h(t_{L,N,i}^{(\sigma,\rho)}) + \eta_1 \Gamma(\alpha) \sum_{j=0}^{N} e_j \Delta_{L,j}^{(\sigma,\rho,\lambda)}(t_{L,N,i}^{(\sigma,\rho)}) + \eta_2 \int_0^1 k(t_{L,N,i}^{(\sigma,\rho)}, s) \sum_{j=0}^{N} e_j \mathcal{P}_{L,j}^{(\sigma,\rho,\lambda)}(s) ds \tag{37}$$

and

$$\sum_{j=0}^{N} e_j \big[\Lambda_{L,j}^{(\sigma,\rho,\lambda)}(t_{L,N,i}^{(\sigma,\rho)}) - \eta_1 \Gamma(\alpha) \Delta_{L,j}^{(\sigma,\rho,\lambda)}(t_{L,N,i}^{(\sigma,\rho)}) - \eta_2 \int_0^1 k(t_{L,N,i}^{(\sigma,\rho)}, s) \mathcal{P}_{L,j}^{(\sigma,\rho,\lambda)}(s) ds \big] = h(t_{L,N,i}^{(\sigma,\rho)}). \tag{38}$$

Joining Equations (25) and (26), we can write:

$$\sum_{j=0}^{N} e_j \mathcal{P}_{L,j}^{(\sigma,\rho,\lambda)}(0) = \sum_{j=0}^{N} (-1)^j \frac{\Gamma(j+\rho+1)}{\Gamma(\rho+1)\, j!} e_j = d. \tag{39}$$

Finally, from Equations (38) and (39) we get a system of $N+1$ algebraic equations:

$$\begin{cases} \sum\limits_{j=0}^{N} (-1)^j \frac{\Gamma(j+\rho+1)}{\Gamma(\rho+1)\, j!} e_j = d, \\ \sum\limits_{j=0}^{N} e_j \big[\Lambda_{L,j}^{(\sigma,\rho,\lambda)}(t_{L,N,i}^{(\sigma,\rho)}) - \eta_1 \Gamma(\alpha) \Delta_{L,j}^{(\sigma,\rho,\lambda)}(t_{L,N,i}^{(\sigma,\rho)}) - \eta_2 \int_0^1 k(t_{L,N,i}^{(\sigma,\rho)}, s) \mathcal{P}_{L,j}^{(\sigma,\rho,\lambda)}(s) ds \big] = h(t_{L,N,i}^{(\sigma,\rho)}) \end{cases} \tag{40}$$

to compute $\chi_N(t)$.

4. Algorithm for Solving VO-FIDE-WSK with Nonlocal Boundary Conditions

In this section, we present a modified spectral algorithm for solving the VO-FIDE-WSK

$$D^{\delta(t)} \chi(t) = h(t) + \int_0^t \frac{\chi(s)}{(t-s)^\alpha} ds, \tag{41}$$

with the nonlocal boundary conditions:

$$\chi(0) + \gamma \chi(1) + \lambda \int_a^b \phi(s) \chi(s) ds = d_1. \tag{42}$$

Following the information included in the previous subsections, we obtain the system of algebraic equations:

$$\begin{cases} \sum\limits_{j=0}^{N} e_j \Big[\mathcal{P}_{L,j}^{(\sigma,\rho,\lambda)}(0) + \gamma_j \mathcal{P}_{L,j}^{(\sigma,\rho,\lambda)}(1) + \lambda \big(\int\limits_a^b \phi(s) \mathcal{P}_{L,j}^{(\sigma,\rho,\lambda)}(s) \big) \Big] = d_1 \\ \sum\limits_{j=0}^{N} e_j \Big[\Lambda_{L,j}^{(\sigma,\rho,\lambda)}(t_{L,N,i}^{(\sigma,\rho)}) - \eta_1 \Gamma(\alpha) \Delta_{L,j}^{(\sigma,\rho,\lambda)}(t_{L,N,i}^{(\sigma,\rho)}) \Big] = h(t_{L,N,i}^{(\sigma,\rho)}) \end{cases}. \tag{43}$$

After the coefficients e_j are determined, it is straightforward to compute the approximate solution $\chi_N(t)$ at any value of t in the given domain.

5. Illustrative Examples

The proposed method is compared with alternative approaches to solve VO-FIDE-WSK equations. Its accuracy and effectiveness is illustrated. We must note that in all examples given below we take $L = 1$.

Example 1. *We consider the VO-FIDE-WSK:*

$$\begin{aligned} D^{\delta(t)}\chi(t) =& \frac{1}{2}\int_0^t \frac{\chi(s)}{(t-s)^{\frac{1}{2}}}ds + \frac{1}{3}\int_0^1 (t-s)\chi(s)ds - \frac{2t^{2-\delta(t)}(\delta(t)-3t-3)}{\Gamma(4-\delta(t))} - \\ & \frac{1}{105}8(6t+7)t^{5/2} - \frac{7t}{36} + \frac{3}{20}, \end{aligned} \tag{44}$$

with supplementary condition:

$$\chi(0) = 0. \tag{45}$$

The exact solution [13,19] is $\chi(t) = t^2 + t^3$, when $\delta(t) = \sin(t)$ and $\lambda = \frac{1}{2}$.

Table 1 summarizes and compares the absolute error, $E(t)$, at $t = \{0, \frac{1}{6}, \frac{2}{6}, \frac{3}{6}, \frac{4}{6}, \frac{5}{6}\}$, between the exact and approximate solutions of the proposed method (for $N = 6$) with those reported in references [13] (for $k = 4$) and [19] (for $N = 24$).

Table 1. The $E(t)$ of Example 1 for $(\sigma, \rho) = (0, \frac{1}{2})$, $\lambda = \frac{1}{2}$.

	SCW [13]	**CAS [19]**	**New Method**
t	$k = 4$	$N = 24$	$N = 6$
0	1.4395×10^{-4}	6.3491×10^{-3}	1.3878×10^{-17}
$\frac{1}{6}$	2.2617×10^{-4}	1.1460×10^{-2}	1.0408×10^{-16}
$\frac{2}{6}$	5.9826×10^{-4}	9.6982×10^{-3}	8.3267×10^{-17}
$\frac{3}{6}$	1.1274×10^{-3}	2.9504×10^{-3}	2.7756×10^{-17}
$\frac{4}{6}$	1.4961×10^{-3}	9.6733×10^{-3}	1.8041×10^{-16}
$\frac{5}{6}$	2.2056×10^{-3}	2.9484×10^{-2}	1.9429×10^{-16}

Figures 1 and 2 depict $E(t)$ and the exact and approximate solutions, respectively, obtained by the proposed method for $N = 6$. The results show good accuracy with a limited number of nodes.

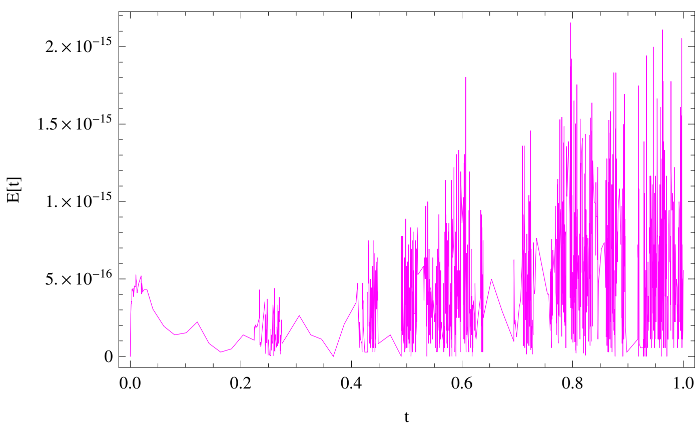

Figure 1. The $E(t)$ of Example 1 for $N = 6$, $(\sigma, \rho) = (0, \frac{1}{2})$, $\lambda = \frac{1}{2}$.

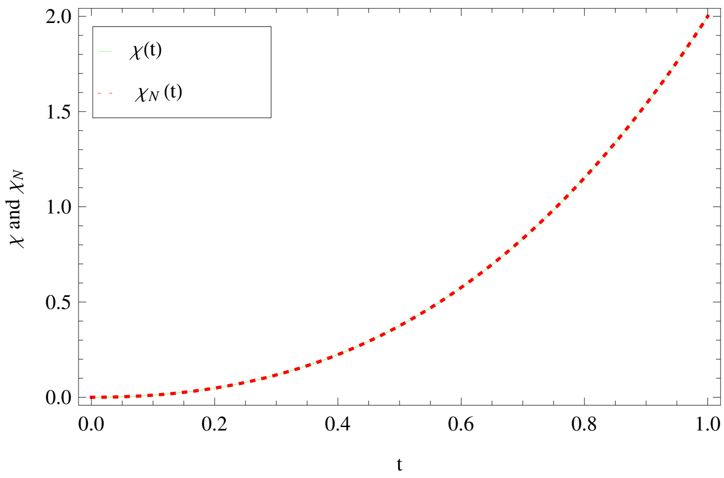

Figure 2. The approximate and exact solutions, $\chi_N(t)$ and $\chi(t)$, of Example 1 for $N = 6$ $(\sigma, \rho) = (0, \frac{1}{2})$, $\lambda = \frac{1}{2}$.

Example 2. *We solve the VO-FIDE-WSK:*

$$\begin{aligned} D^{\delta(t)}\chi(t) =& \frac{1}{4}\int_0^t \frac{\chi(s)}{(t-s)^{\frac{1}{4}}}ds + \frac{1}{7}\int_0^1 e^{(t+s)}\chi(s)ds + \frac{t^{1-\delta(t)}(\delta(t)+2t-2)}{\Gamma(3-\delta(t))} - \\ & \frac{4}{231}(11-8t)t^{7/4} - \frac{1}{7}(e-3)e^t, \end{aligned} \tag{46}$$

with condition:

$$\chi(0) = 0. \tag{47}$$

The exact solution of the equation is $\chi(t) = t^2 - t$ for $\lambda = \frac{1}{2}$ and $\delta(t) = 0.15t$.

Table 2 lists the values of $E(t)$ obtained with $N = 4$ for $(\sigma, \rho) = (0, -\frac{1}{2})$, $(\sigma, \rho) = (0, 0)$ and $\lambda = \frac{1}{2}$. Figures 3 and 4 illustrate the $E(t)$ dynamics and compare the exact and approximate solutions, respectively. We can conclude that the method leads to very accurate solutions.

Table 2. The $E(t)$ of Example 2 obtained with $N = 4$ for $(\sigma, \rho) = (0, -\frac{1}{2})$, $(\sigma, \rho) = (0, 0)$ and $\lambda = \frac{1}{2}$.

	New Method at $N = 4$	
t	$\sigma = 0,\ \rho = -\frac{1}{2}$	$\sigma = \rho = 0$
0	5.2042×10^{-18}	2.0817×10^{-17}
0.1	1.3488×10^{-15}	9.2548×10^{-16}
0.2	5.8287×10^{-16}	4.5103×10^{-16}
0.3	3.3307×10^{-16}	1.2490×10^{-16}
0.4	2.7756×10^{-16}	5.5511×10^{-17}
0.5	5.2736×10^{-16}	8.3267×10^{-17}
0.6	8.3961×10^{-16}	2.4980×10^{-16}
0.7	1.2438×10^{-15}	1.4572×10^{-16}
0.8	1.2906×10^{-15}	6.3144×10^{-16}
0.9	1.1657×10^{-15}	8.0491×10^{-16}

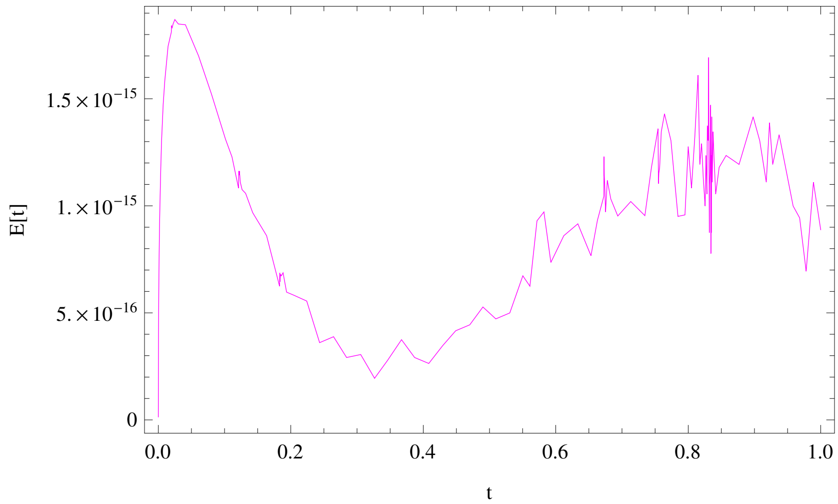

Figure 3. The $E(t)$ of Example 2 for $N = 4$, $(\sigma, \rho) = (0, 0)$ and $\lambda = \frac{1}{2}$.

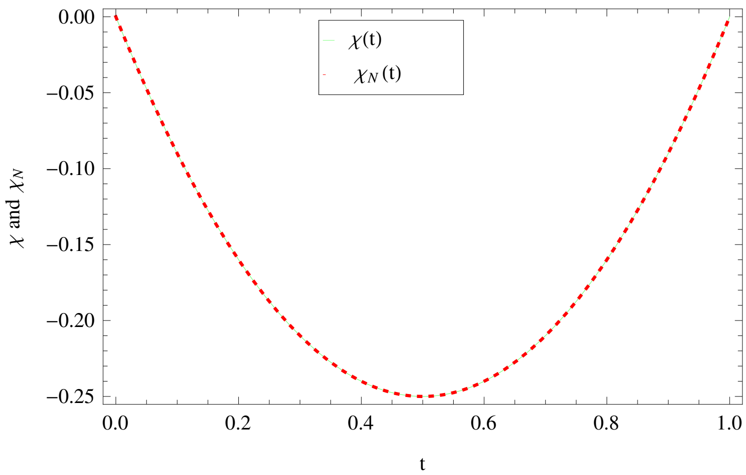

Figure 4. The approximate and the exact solutions, $\chi_N(t)$ and $\chi(t)$, of Example 2 for $N = 4$, $(\sigma, \rho) = (0, 0)$ and $\lambda = \frac{1}{2}$.

Example 3. *We solve the VO-FIDE-WSK:*

$$D^{\delta(t)}\chi(t) = \int_0^t \frac{\chi(s)}{(t-s)^{\frac{1}{2}}}ds + \int_0^1 (t^2 + \cos(s))\chi(s)ds - \frac{1}{15}\Big(16\sqrt{t} + 5\Big)t^2 + \frac{2t^{2-t\sin(t)}}{\Gamma(3 - t\sin(t))} + \sin(1) - 2\cos(1), \tag{48}$$

with initial condition:

$$\chi(0) = 0. \tag{49}$$

The exact solution is $\chi(t) = t^2$*, when* $\lambda = \frac{1}{2}$.

The solution of (48) is obtained by applying the new technique. The $E(t)$ is shown in Table 3 when $N = 4$ and for $(\sigma, \rho) = (0, 0)$ and $(\sigma, \rho) = (\frac{1}{2}, 0)$. Figures 5 and 6 depict the $E(t)$ dynamics and compare the approximate and exact solutions, respectively. As before, we verify the good accuracy provided by the method.

Table 3. The $E(t)$ of Example 3 obtained with $N = 4$ for $(\sigma, \rho) = (0, 0)$ and $(\sigma, \rho) = (\frac{1}{2}, 0)$, and $\lambda = \frac{1}{2}$.

	New Method at $N = 4$	
t	$\sigma = \rho = 0$	$\sigma = \frac{1}{2}, \rho = 0$
0	0	0
$\frac{1}{6}$	2.7756×10^{-17}	7.6328×10^{-17}
$\frac{2}{6}$	2.7756×10^{-17}	1.9429×10^{-16}
$\frac{3}{6}$	6.9389×10^{-17}	4.4409×10^{-16}
$\frac{4}{6}$	1.2837×10^{-16}	5.2736×10^{-16}
$\frac{5}{6}$	1.3878×10^{-16}	6.8001×10^{-16}

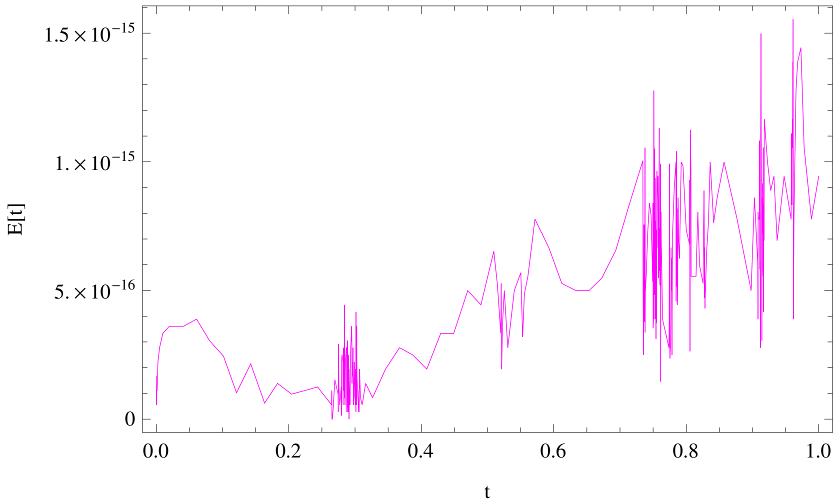

Figure 5. The $E(t)$ of Example 3 for $N = 4$, $(\sigma, \rho) = (\frac{1}{2}, 0)$ and $\lambda = \frac{1}{2}$.

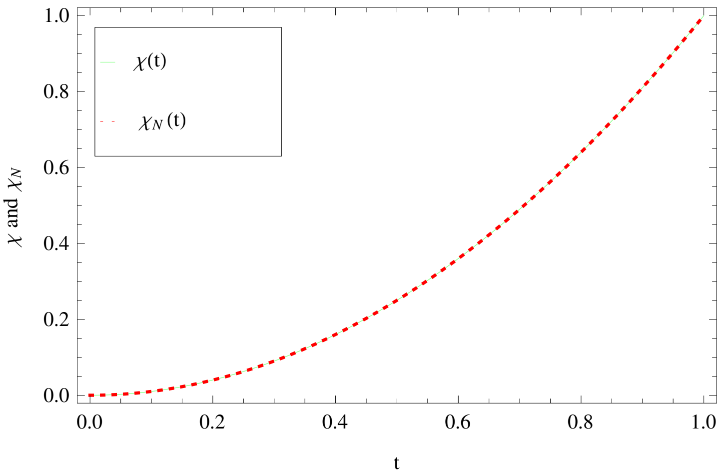

Figure 6. The approximate and exact solutions, $\chi_N(t)$ and $\chi(t)$, of Example 3 for $N = 4$, $(\sigma, \rho) = (\frac{1}{2}, 0)$ and $\lambda = \frac{1}{2}$.

Example 4. *We solve the VO-FIDE-WSK:*

$$D^{\delta(t)}\chi(t) = \mu(t)\chi(t) + \int_0^t \frac{\chi(s)}{(t-s)^{\frac{1}{2}}} ds + \frac{1}{35} t^{11/6} \left(22 - \frac{35\sqrt{\pi}\Gamma\left(\frac{7}{3}\right)}{\Gamma\left(\frac{17}{6}\right)}\right) + t^{-\delta(t)} \left(\frac{t^{4/3}\Gamma\left(\frac{7}{3}\right)}{\Gamma\left(\frac{7}{3} - \delta(t)\right)} + \frac{6t^3}{\Gamma(4 - \delta(t))}\right), \tag{50}$$

with supplementary condition:

$$\chi(0) = 0. \quad (51)$$

The exact solution of the equation [12,15] is $\chi(t) = t^3 + t^{\frac{4}{3}}$ *for* $\delta(t) = \sin(t)$, $\lambda = \frac{1}{2}$, *and* $\mu = -\frac{22}{35}t^{\frac{1}{2}}$.

To assess the rate of convergence, we list maximum absolute errors (MAE) in Table 4. The results show that at different values of N the method has superior accuracy than those addressed in references [12,15]. Figures 7 and 8 depict $E(t)$ for $N = 20$ and $\lambda = \frac{1}{2}$ and $\lambda = \frac{2}{3}$. Figures 9 and 10 show the MAE at various values of N, and $\lambda = \frac{1}{2}$ and $\lambda = \frac{2}{3}$. The results reveal good accuracy and exponential convergence of the method.

Table 4. The MAE of Example 4 for various values of N, $\lambda = \frac{1}{2}$, $\lambda = \frac{2}{3}$ and $(\sigma, \rho) = (0, \frac{1}{2})$, and their comparison with those obtained in [12,15].

	Operational Matrix [12]	**Operational Tau Method** [15]	**New Method**	
N			$\lambda = \frac{1}{2}$	$\lambda = \frac{2}{3}$
2	1.34×10^{-2}	1.34×10^{-2}	2.54×10^{-1}	1.11×10^{-1}
4	5.14×10^{-4}	5.14×10^{-4}	8.67×10^{-3}	1.14×10^{-3}
6	1.56×10^{-4}	1.56×10^{-4}	2.76×10^{-5}	8.28×10^{-6}
8	6.46×10^{-5}	6.46×10^{-5}	5.93×10^{-6}	3.99×10^{-7}
16	–	7.38×10^{-6}	4.91×10^{-8}	5.54×10^{-10}
18	–	4.62×10^{-6}	3.69×10^{-8}	1.37×10^{-10}
20	–	2.85×10^{-6}	1.16×10^{-8}	7.63×10^{-11}

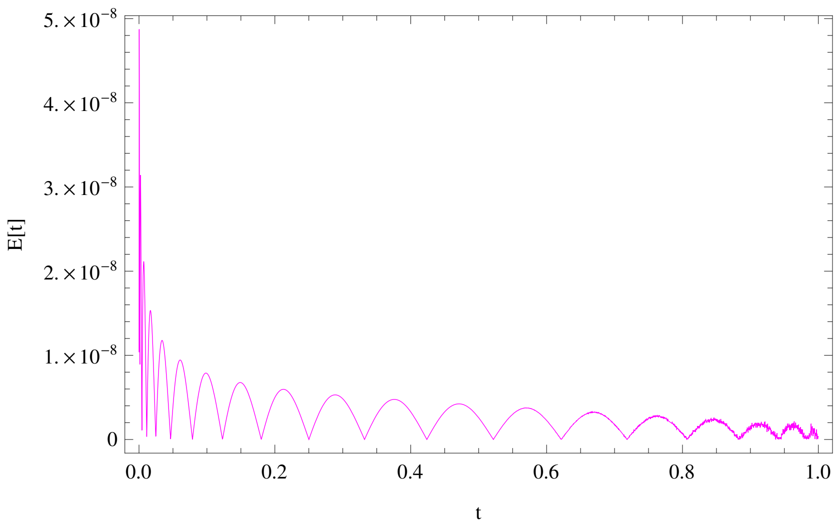

Figure 7. The $E(t)$ of Example 4 for $N = 20$, $\lambda = \frac{1}{2}$ and $(\sigma, \rho) = (0, \frac{1}{2})$.

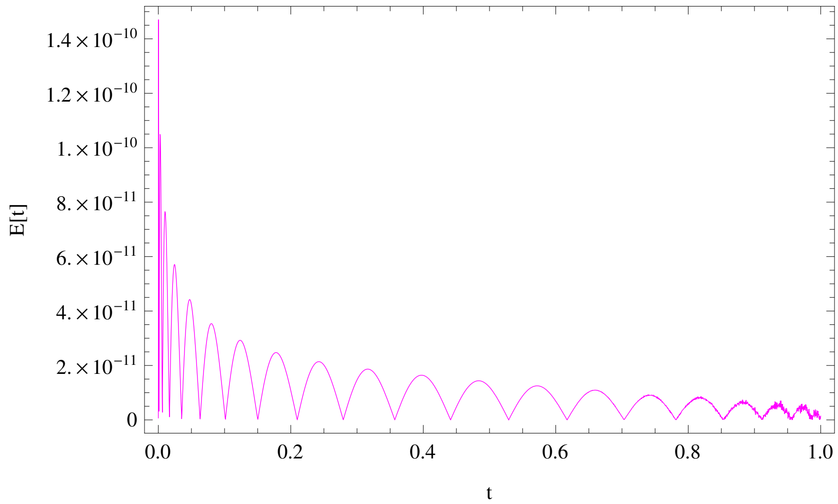

Figure 8. The $E(t)$ of Example 4 for $N = 20$, $\lambda = \frac{2}{3}$ and $(\sigma, \rho) = (0, \frac{1}{2})$.

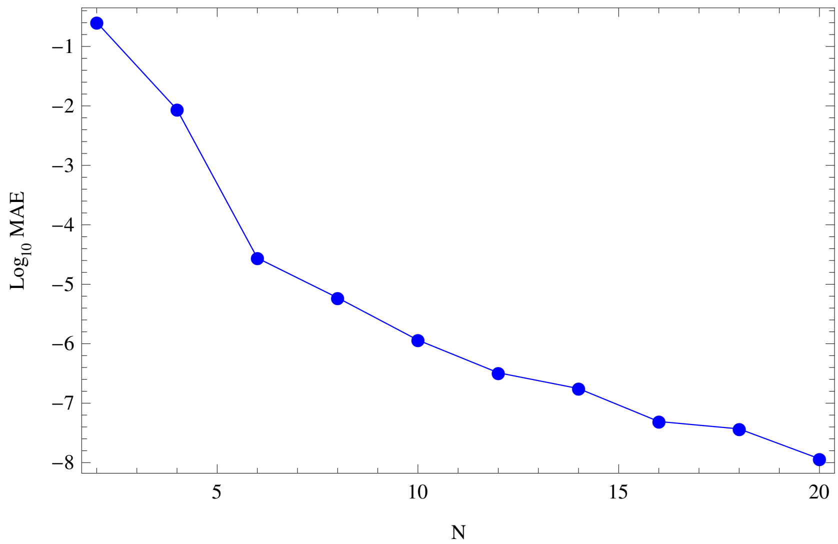

Figure 9. The MAE of Example 4, with $\lambda = \frac{1}{2}$ and $(\sigma, \rho) = (0, \frac{1}{2})$.

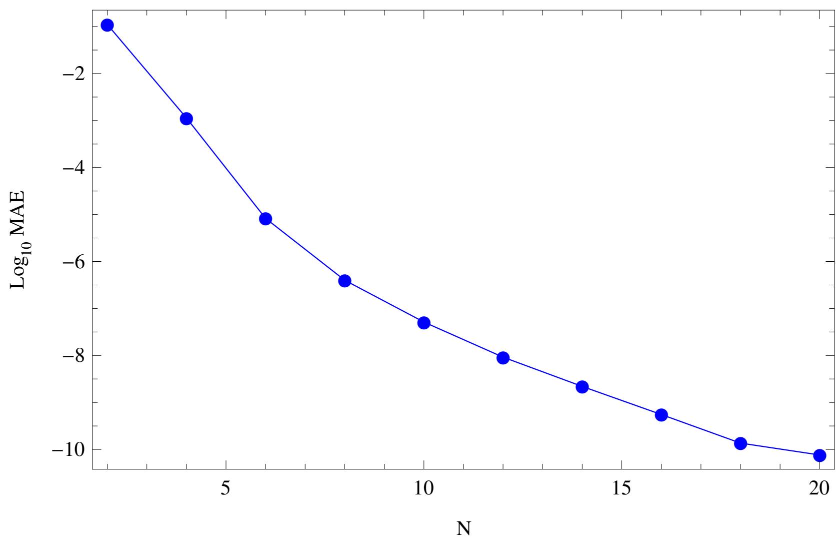

Figure 10. The MAE for Example 4, with $\lambda = \frac{2}{3}$ and $(\sigma, \rho) = (0, \frac{1}{2})$.

Example 5. *In this example, we address the VO-FIDE-WSK*

$$D^{\delta(t)}\chi(t) = \int_0^t \frac{\chi(t)}{\sqrt{t-s}}ds + \frac{35}{128}\left(\frac{24\sqrt{\pi}t^{\frac{7}{2}-\delta(t)}}{\Gamma\left(\frac{9}{2}-\delta(t)\right)} - \pi t^4\right), \tag{52}$$

with the nonlocal condition:

$$\chi(0) + \chi(1) - 3\int_0^1 s^2\chi(s)ds = \frac{7}{13}. \tag{53}$$

The exact solution is a non-smooth $\chi(t) = t^{3.5}$ *with* $\delta(t) = \frac{t}{3}$.

The values of the MAE for Example 5 subject to the nonlocal condition (53) are listed in Table 5. Figures 11 and 12 depict the error $E(t)$ for $N = 8$, $\lambda = \frac{1}{2}$, $(\sigma, \rho) = (0, \frac{1}{2})$, and $\delta(t) = \frac{t}{3}$ and $\delta(t) = t\sin(t)$, respectively. We verify that the method yields accurate results.

Table 5. The MAE of Example 5 for various values of N, $\lambda = \frac{1}{2}$, $(\sigma, \rho) = (0, \frac{1}{2})$, and $\delta(t) = \{\frac{t}{3}, t\sin(t)\}$.

N	$\frac{t}{3}$	$t\sin(t)$
2	3.330×10^{-1}	3.552×10^{-1}
4	1.625×10^{-2}	1.950×10^{-2}
6	1.476×10^{-4}	1.553×10^{-4}
8	3.137×10^{-15}	2.7113×10^{-15}

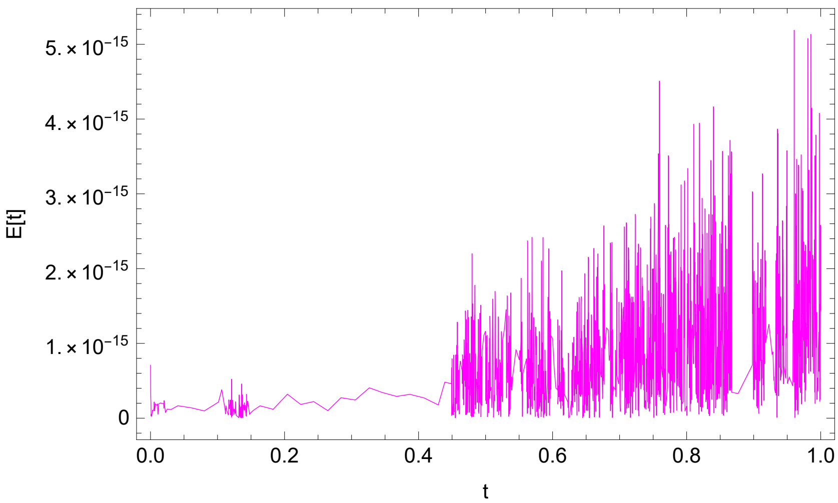

Figure 11. The $E(t)$ of Example 5 for $N = 8$, $\lambda = \frac{1}{2}$, $(\sigma, \rho) = (0, \frac{1}{2})$ and $\delta(t) = \frac{t}{3}$.

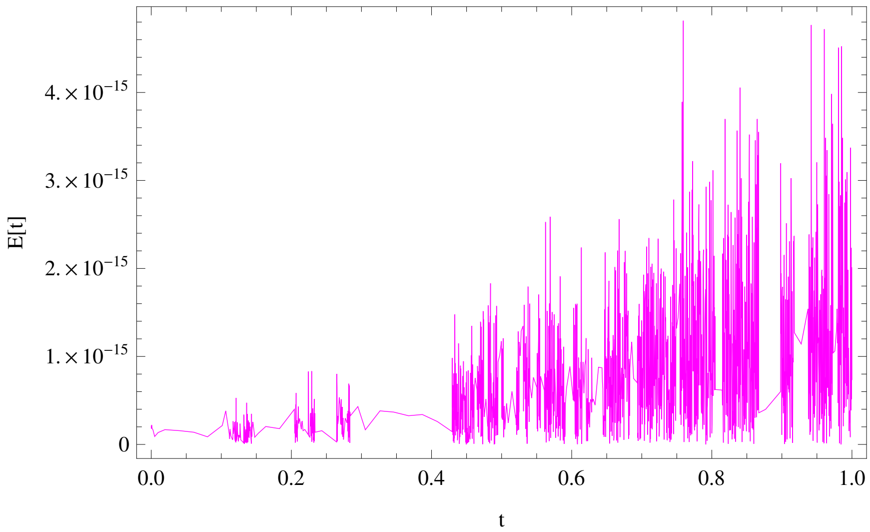

Figure 12. The $E(t)$ of Example 5 for $N = 8$, $\lambda = \frac{1}{2}$, $(\sigma, \rho) = (0, \frac{1}{2})$, and $\delta(t) = t\sin(t)$.

6. Discussion

The examples presented in Section 5 can be summarized as follows:

Case I: Exs. 1, 2, 3 and 5 (with $N = 8$).

In these examples, for $\lambda = \frac{1}{2}$, $\chi(t)$ is a polynomial in t, and N is greater than, or equal to, twice the degree of the polynomial $\chi(t)$. Therefore, the exact solution $\chi(t)$ belongs to the vector space $\mathcal{F}_N$, meaning that $\chi_N(t) = \chi(t)$, or, equivalently, $E(t) = 0$. The numerical decimal errors $E(t)$ shown in Tables 1–3 and 5 for these cases are not due to the algorithm given in Equation (43), but from the decimal approximation of this expression. It must be mentioned that the algorithm gives the exact solution under the conditions adopted.

Case II: Exs. 4 and 5 (with $N = 2, 4, 6$).

In these examples, we verify that $\chi(t)$ does not belong to the vector space $\mathcal{F}_N$. Thus, the errors $E(t)$ given in Tables 4 and 5 (with $N = 2, 4, 6$) are much larger than the ones of Case I.

Regarding Ex. 4, we verify that Equation (50), as well as the VO-FIDE-WSK (24), is linear in the unknown function $\chi(t)$ with the non-homogeneous term $h(t)$. The exact solution $\chi(t) = t^3 + t^{\frac{4}{3}}$ is a linear combination of two power functions t^3 and $t^{\frac{4}{3}}$, and $h_A(t) = t^{-\delta(t)} \frac{6t^3}{\Gamma(4-\delta(t))}$ and $h_B(t) = \frac{1}{35} t^{11/6} \left(22 - \frac{35\sqrt{\pi}\Gamma(\frac{7}{3})}{\Gamma(\frac{17}{6})}\right) + t^{-\delta(t)} \frac{t^{\frac{4}{3}}\Gamma(\frac{7}{3})}{\Gamma(\frac{7}{3}-\delta(t))}$, respectively. For $\lambda = \frac{1}{2}$ and $h(t) = h_A(t)$, we have $\chi(t) = t^3$ and, with $N \geq 6$, it yields $\chi_N(t) = \chi(t)$ (this is well illustrated by examples in Case I). Therefore, the function $\chi(t) = t^3$ does not contribute to the error term for the approximate solution. In this case, it turns out that $\chi(t) = t^{\frac{4}{3}}$ does not belong to $\mathcal{F}_N$ for any N, and the approximate solution $\chi_N(t)$ for $\chi(t) = t^{\frac{4}{3}}$ with $h(t) = h_B(t)$ is the main concern. For $\lambda = \frac{2}{3}$ and $h(t) = h_B(t)$, we get $\chi(t) = t^{\frac{4}{3}}$ and, with $N \geq 4$, it results in $\chi_N(t) = \chi(t)$. Thus, the function $\chi(t) = t^{\frac{4}{3}}$ does not contribute to the error term for the approximate solution. In this case, it turns out that $\chi(t) = t^3$ does not belong to $\mathcal{F}_N$ for any N, and the approximate solution $\chi_N(t)$ for $\chi(t) = t^3$ with $h(t) = h_A(t)$ is now the main concern.

7. Conclusions

This paper proposed a new numerical approach based on the FSJ-G-C method and R-LF operators to solve VO-FIDE-WSK subject to initial conditions. The novel algorithm reduces the solution of the original problem to a system of algebraic equations that is solved by any suitable procedure. Four numerical examples revealed that the proposed scheme is efficient and accurate when compared with alternatives reported in the literature.

Author Contributions: Data curation, M.A.A., A.Z.M.A., M.M.B., I.H. and A.M.L.; Formal analysis, M.A.A., A.Z.M.A., M.M.B., I.H. and A.M.L.; Funding acquisition, M.A.A.; Methodology, M.A.A., A.Z.M.A. and A.M.L.; Software, M.A.A., A.Z.M.A., I.H. and A.M.L.; Writing—original draft, M.A.A., A.Z.M.A., M.M.B., I.H. and A.M.L.; Writing— review and editing, M.A.A., A.Z.M.A., A.M.L. and I.H. All authors contributed equally. All authors have read and agreed to the published version of the manuscript.

Funding: The authors extend their appreciation to the Deanship of Scientific Research at Imam Mohammad Ibn Saud Islamic University for funding this work through Research Group no. RG-21-09-05.

Institutional Review Board Statement: Not applicable.

Informed Consent Statement: Not applicable.

Data Availability Statement: Not applicable.

Conflicts of Interest: The authors declare no conflict of interest.

References

1. Abdelkawy, M.A.; Ezz-Eldien, S.S.; Amin, A.Z. A Jacobi spectral collocation scheme for solving Abel's integral equations. *Prog. Fract. Differ. Appl.* **2015**, *1*, 1–14.
2. Eslahchi, M.; Dehghan, M.; Parvizi, M. Application of the collocation method for solving nonlinear fractional integro-differential equations. *J. Comput. Appl. Math.* **2014**, *257*, 105–128. [CrossRef]
3. Baleanu, D.; Diethelm, K.; Scalas, E.; Trujillo, J.J. *Fractional Calculus: Models and Numerical Methods*; World Scientific: Singapore, 2012; Volume 3.
4. Bhrawy, A.H.; Abdelkawy, M.A. A fully spectral collocation approximation for multi-dimensional fractional Schrödinger equations. *J. Comput. Phys.* **2015**, *294*, 462–483. [CrossRef]
5. Zayernouri, M.; Karniadakis, G.E. Exponentially accurate spectral and spectral element methods for fractional ODEs. *J. Comput. Phys.* **2014**, *257*, 460–480. [CrossRef]
6. Yang, X.J.; Gao, F.; Machado, J.T.; Baleanu, D. A new fractional derivative involving the normalized sinc function without singular kernel. *Eur. Phys. J. Spec. Top.* **2017**, *226*, 3567–3575. [CrossRef]
7. Yang, X.J.; Machado, J.; Nieto, J.J. A new family of the local fractional PDEs. *Fundam. Informaticae* **2017**, *151*, 63–75. [CrossRef]
8. Yang, X.J.; Abdel-Aty, M.; Cattani, C. A new general fractional-order derivataive with Rabotnov fractional-exponential kernel applied to model the anomalous heat transfer. *Therm. Sci.* **2019**, *23*, 1677–1681. [CrossRef]
9. Chen, L.; Pan, W.; Wu, R.; Tenreiro Machado, J.; Lopes, A.M. Design and implementation of grid multi-scroll fractional-order chaotic attractors. *Chaos Interdiscip. J. Nonlinear Sci.* **2016**, *26*, 084303. [CrossRef]
10. Lopes, A.M.; Machado, J.T. Modeling vegetable fractals by means of fractional-order equations. *J. Vib. Control* **2016**, *22*, 2100–2108. [CrossRef]
11. Momani, S.; Noor, M.A. Numerical methods for fourth-order fractional integro-differential equations. *Appl. Math. Comput.* **2006**, *182*, 754–760. [CrossRef]
12. Nemati, S.; Sedaghat, S.; Mohammadi, I. A fast numerical algorithm based on the second kind Chebyshev polynomials for fractional integro-differential equations with weakly singular kernels. *J. Comput. Appl. Math.* **2016**, *308*, 231–242. [CrossRef]
13. Wang, Y.; Zhu, L. SCW method for solving the fractional integro-differential equations with a weakly singular kernel. *Appl. Math. Comput.* **2016**, *275*, 72–80. [CrossRef]
14. Zhao, J.; Xiao, J.; Ford, N.J. Collocation methods for fractional integro-differential equations with weakly singular kernels. *Numer. Algorithms* **2014**, *65*, 723–743. [CrossRef]
15. Mokhtary, P. Numerical analysis of an operational Jacobi Tau method for fractional weakly singular integro-differential equations. *Appl. Numer. Math.* **2017**, *121*, 52–67. [CrossRef]
16. Yi, M.; Wang, L.; Huang, J. Legendre wavelets method for the numerical solution of fractional integro-differential equations with weakly singular kernel. *Appl. Math. Model.* **2016**, *40*, 3422–3437. [CrossRef]
17. Pedas, A.; Tamme, E.; Vikerpuur, M. Spline collocation for fractional weakly singular integro-differential equations. *Appl. Numer. Math.* **2016**, *110*, 204–214. [CrossRef]
18. Bhrawy, A.H.; Abdelkawy, M.A.; Baleanu, D.; Amin, A.Z. A spectral technique for solving two-dimensional fractional integral equations with weakly singular kernel. *Hacet. J. Math. Stat.* **2018**, *47*, 553–566. [CrossRef]
19. Yi, M.; Huang, J. CAS wavelet method for solving the fractional integro-differential equation with a weakly singular kernel. *Int. J. Comput. Math.* **2015**, *92*, 1715–1728. [CrossRef]
20. Doha, E.H.; Abdelkawy, M.A.; Amin, A.; Lopes, A.M. Shifted Jacobi–Gauss-collocation with convergence analysis for fractional integro-differential equations. *Commun. Nonlinear Sci. Numer. Simul.* **2019**, *72*, 342–359. [CrossRef]
21. Xu, Y.; Suat, E.V. A finite difference technique for solving variable-order fractional integro-differential equations. *Bull. Iran. Math. Soc.* **2014**, *40*, 699–712.
22. Chen, Y.M.; Wei, Y.Q.; Liu, D.Y.; Yu, H. Numerical solution for a class of nonlinear variable order fractional differential equations with Legendre wavelets. *Appl. Math. Lett.* **2015**, *46*, 83–88. [CrossRef]

23. Sun, K.; Zhu, M. Numerical algorithm to solve a class of variable order fractional integral-differential equation based on Chebyshev polynomials. *Math. Probl. Eng.* **2015**, *2015*, 902161. [CrossRef]
24. Chen, Y.; Liu, L.; Li, B.; Sun, Y. Numerical solution for the variable order linear cable equation with Bernstein polynomials. *Appl. Math. Comput.* **2014**, *238*, 329–341. [CrossRef]
25. Bhrawy, A.; Zaky, M. Numerical simulation for two-dimensional variable-order fractional nonlinear cable equation. *Nonlinear Dyn.* **2015**, *80*, 101–116. [CrossRef]
26. Tavares, D.; Almeida, R.; Torres, D.F. Caputo derivatives of fractional variable order: Numerical approximations. *Commun. Nonlinear Sci. Numer. Simul.* **2016**, *35*, 69–87. [CrossRef]
27. Atangana, A. On the stability and convergence of the time-fractional variable order telegraph equation. *J. Comput. Phys.* **2015**, *293*, 104–114. [CrossRef]
28. Zhang, H.; Liu, F.; Zhuang, P.; Turner, I.; Anh, V. Numerical analysis of a new space–time variable fractional order advection–dispersion equation. *Appl. Math. Comput.* **2014**, *242*, 541–550. [CrossRef]
29. Zayernouri, M.; Karniadakis, G.E. Fractional spectral collocation methods for linear and nonlinear variable order FPDEs. *J. Comput. Phys.* **2015**, *293*, 312–338. [CrossRef]
30. Abd-Elkawy, M.A.; Alqahtani, R.T. Space-time spectral collocation algorithm for the variable-order Galilei invariant advection diffusion equations with a nonlinear source term. *Math. Model. Anal.* **2017**, *22*, 1–20. [CrossRef]
31. Zhao, X.; Sun, Z.Z.; Karniadakis, G.E. Second-order approximations for variable order fractional derivatives: Algorithms and applications. *J. Comput. Phys.* **2015**, *293*, 184–200. [CrossRef]
32. Chen, S.; Liu, F.; Burrage, K. Numerical simulation of a new two-dimensional variable-order fractional percolation equation in non-homogeneous porous media. *Comput. Math. Appl.* **2014**, *68*, 2133–2141. [CrossRef]
33. Alikhanov, A.A. Numerical methods of solutions of boundary value problems for the multi-term variable-distributed order diffusion equation. *Appl. Math. Comput.* **2015**, *268*, 12–22. [CrossRef]
34. Sweilam, N.H.; Assiri, T.A.R. Numerical simulations for the space-time variable order nonlinear fractional wave equation. *J. Appl. Math.* **2013**, *2013*, 586870. [CrossRef]
35. Razminia, A.; Dizaji, A.F.; Majd, V.J. Solution existence for non-autonomous variable-order fractional differential equations. *Math. Comput. Model.* **2012**, *55*, 1106–1117. [CrossRef]
36. Liu, J.; Li, X.; Wu, L. An operational matrix technique for solving variable order fractional differential-integral equation based on the second kind of Chebyshev polynomials. *Adv. Math. Phys.* **2016**, *2016*, 6345978. [CrossRef]
37. Chen, C.M.; Liu, F.; Burrage, K. Numerical analysis for a variable-order nonlinear cable equation. *J. Comput. Appl. Math.* **2011**, *236*, 209–224. [CrossRef]
38. Lin, R.; Liu, F.; Anh, V.; Turner, I. Stability and convergence of a new explicit finite-difference approximation for the variable-order nonlinear fractional diffusion equation. *Appl. Math. Comput.* **2009**, *212*, 435–445. [CrossRef]
39. Bhrawy, A.H.; Alofi, A.S. A Jacobi–Gauss collocation method for solving nonlinear Lane–Emden type equations. *Commun. Nonlinear Sci. Numer. Simul.* **2012**, *17*, 62–70. [CrossRef]
40. Bhrawy, A.; Abdelkawy, M.; Machado, J.T.; Amin, A. Legendre–Gauss–Lobatto collocation method for solving multi-dimensional Fredholm integral equations. *Comput. Math. Appl.* **2016**, *4*, 1–13. [CrossRef]
41. Bhrawy, A.H. A Jacobi–Gauss–Lobatto collocation method for solving generalized Fitzhugh–Nagumo equation with time-dependent coefficients. *Appl. Math. Comput.* **2013**, *222*, 255–264. [CrossRef]
42. Abdelkawy, M.A.; Amin, A.Z.; Bhrawy, A.H.; Machado, J.A.T.; Lopes, A.M. Jacobi collocation approximation for solving multi-dimensional Volterra integral equations. *Int. J. Nonlinear Sci. Numer. Simul.* **2017**, *18*, 411–425. [CrossRef]
43. Doha, E.; Bhrawy, A.; Baleanu, D.; Hafez, R. A new Jacobi rational–Gauss collocation method for numerical solution of generalized pantograph equations. *Appl. Numer. Math.* **2014**, *77*, 43–54. [CrossRef]
44. Ghoreishi, F.; Yazdani, S. An extension of the spectral Tau method for numerical solution of multi-order fractional differential equations with convergence analysis. *Comput. Math. Appl.* **2011**, *61*, 30–43. [CrossRef]
45. Mokhtary, P.; Ghoreishi, F. The L^2-convergence of the Legendre spectral Tau matrix formulation for nonlinear fractional integro differential equations. *Numer. Algorithms* **2011**, *58*, 475–496. [CrossRef]
46. Bhrawy, A.H.; Doha, E.H.; Baleanu, D.; Ezz-Eldien, S.S. A spectral tau algorithm based on Jacobi operational matrix for numerical solution of time fractional diffusion-wave equations. *J. Comput. Phys.* **2015**, *293*, 142–156. [CrossRef]
47. Doha, E.H.; Bhrawy, A.H. An efficient direct solver for multidimensional elliptic Robin boundary value problems using a Legendre spectral-Galerkin method. *Comput. Math. Appl.* **2012**, *64*, 558–571. [CrossRef]
48. Chen, F.; Shen, J. Efficient spectral-Galerkin methods for systems of coupled second-order equations and their applications. *J. Comput. Phys.* **2012**, *231*, 5016–5028. [CrossRef]
49. Shen, J. A new dual-Petrov-Galerkin method for third and higher odd-order differential equations: Application to the KDV equation. *SIAM J. Numer. Anal.* **2003**, *41*, 1595–1619. [CrossRef]
50. Doha, E.H.; Bhrawy, A.H.; Hafez, R. A Jacobi–Jacobi dual-Petrov–Galerkin method for third-and fifth-order differential equations. *Math. Comput. Model.* **2011**, *53*, 1820–1832. [CrossRef]
51. Yang, Q.; Yuan, Y. An approximation of semiconductor device by mixed finite element method and characteristics-mixed finite element method. *Appl. Math. Comput.* **2013**, *225*, 407–424.
52. Wen, J.; He, Y. Convergence analysis of a new multiscale finite element method for the stationary Navier–Stokes problem. *Comput. Math. Appl.* **2014**, *67*, 1–25. [CrossRef]

53. Canuto, C.; Hussaini, M.Y.; Quarteroni, A.; Zang, T.A. *Spectral Methods: Fundamentals in Single Domains*; Springer Science & Business Media: New York, NY, USA, 2007.
54. Okuzono, T.; Otsuru, T.; Tomiku, R.; Okamoto, N. A finite-element method using dispersion reduced spline elements for room acoustics simulation. *Appl. Acoust.* **2014**, *79*, 1–8. [CrossRef]
55. Bhrawy, A.H.; Zaky, M.A. Highly accurate numerical schemes for multi-dimensional space variable-order fractional Schrödinger equations. *Comput. Math. Appl.* **2017**, *73*, 1100–1117. [CrossRef]
56. Zaky, M. Correction to: Numerical simulation for two-dimensional variable-order fractional nonlinear cable equation. *Nonlinear Dyn.* **2018**, *94*, 757. [CrossRef]
57. Abdelkawy, M.; Lopes, A.M.; Babatin, M.M. Shifted fractional Jacobi collocation method for solving fractional functional differential equations of variable order. *Chaos Solitons Fractals* **2020**, *134*, 109721. [CrossRef]
58. Abdelkawy, M.; Babatin, M.M.; Lopes, A.M. Highly accurate technique for solving distributed-order time-fractional-sub-diffusion equations of fourth order. *Comput. Appl. Math.* **2020**, *39*, 1–22. [CrossRef]